Acta Mechanica Solida Sinica, Vol. 20, No. 1, March, 2007 ISSN 0894-9166
Published by AMSS Press, Wuhan, China. DOI: 10.1007/s10338-007-0707-z

QUANTIFICATION OF SHEAR DAMAGE EVOLUTION IN ALUMINIUM ALLOY 2024T3 **

Tang Chak-yin[1] **Fan Jianping**[2*1] **Tsui Chi-pong**[1] **Lee Tai-chiu**[1] **Chan Luen-chow**[1] **Rao Bin**[1]
([1] *Department of Industrial and Systems Engineering, The Hong Kong Polytechnic University, Hong Kong, China*)
([2] *School of Civil Engineering and Mechanics, Huazhong University Science and Technology, Wuhan* 430074*, China*)

Received 10 March 2006; revision received 21 November 2006

ABSTRACT Shear damage may occur in the process of metal machining such as blanking and cutting, where localized shear deformation is developed. Experimental findings indicate that microscopic shear damage evolution in aluminium alloy 2024T3 (Al 2024T3) is a multi-stage mechanism, including particle cracking, micro-shear banding, matrix microcracking and coalescence of microcracks. This study is an attempt to use a set of equations to describe the multi-stage shear damage evolution in Al 2024T3. The shear damage variables in terms of multi-couple parameters of a power-law hardening material have been defined. An evolution curve of shearing damage has been calculated from experimental data. The values of the shear damage variable at different stages of damage have also been calculated. By making use of the findings, the relation between the microscopic shear damage evolution and the macroscopic shear response of the material has been discussed.

KEY WORDS shear damage, damage evolution equations, shear band, hardening material, microscopic observation

I. INTRODUCTION

In continuum damage mechanics (CDM), constitutive and damage evolution equations were often established on the basis of thermodynamics[1]. CDM does not provide much information about the detailed mechanism of damage; instead, it focuses on modelling the macroscopic effect of damage. A dissipation potential usually needs to be defined and constructed to establish the constitutive equations. The dissipation potential is different for different materials and/or different types of damage. The construction of an appropriate dissipation potential is not easy. On the other hand, the constitutive and damage evolution equations may also be established experimentally. For the phenomenological approach, a basic theoretical framework has been formed.

A few studies on shear damage have been reported recently. For axial tension, one defines the damage variable as the degradation of the apparent Young's modulus. Similarly, the shear damage variable has been defined as the degradation of the apparent shear modulus, which means the strain equivalence hypothesis is applied in the case of pure shear[2, 3]. The damage of a composite cylinder with hydrostatic pressure is composed of shear damage and dilatation damage[4]. Meanwhile, in studying

* Corresponding author. E-mail: jpfan@public.wh.hb.cn

** Project supported by the Research Grants Council of the Hong Kong Special Administrative Region (No. PolyU 5131/98E).

shear damage the characteristics of damage are worth considering. In analysing the effect of damage on the mechanical properties of human cortical bone, shear damage has been characterised by degradation of the shear modulus[5]. Shear damage has also been defined by the degeneration of shear modulus[6, 7], while isotropic damage is characterised by two independent scalar damage variables; e.g., shear damage and bulk damage[7, 8].

Loland proposed a model to evaluate damage by a given net stress-strain relation and an experimentally determined nominal stress-strain relation[9]. Mazars has proposed a model in which a similar method was applied[10]. In the stress-based definitions of damage, some assumptions [9, 10] are required to determine the effective stress-strain relation.

In general, it is difficult to quantify localised mesoscopic damage by constitutive equations. The purpose of this study is to propose a set of phenomenological equations for describing a multi-stage of shear damage evolution in the shear band of Al 2024T3, which has been widely used in the aerospace industry. Five-stage shear damage evolution equations are constructed in accordance with the damage mechanisms in each stage. The shear damage evolution curve is obtained from evaluating the shear stress-strain characteristics in a shear band. Eventually, the values of damage at different stages are calculated and the shear damage mechanisms of the aluminium alloy are discussed.

II. THE MICROSCOPIC BASIS FOR QUANTIFYING SHEAR DAMAGE

The damage mechanisms of a material are generally attributed to the effect of the initiation and growth of microdefects, that are usually reflected by degradation of macroscopic properties. Microcracks and microvoids are two common microdefects in metals. The nucleation, coalescence and propagation of microdefects are the predominant mechanisms in metal damage. In addition to experimental investigations, numerical simulations of material damage have been quickly developed in recent years. In most cases, a theoretical model describing the nucleation and propagation of the microdefects is verified either experimentally or numerically.

A previous experimental investigation[11] by the author and co-workers studying the shear damage mechanism of Al 2024T3 forms the knowledge base for this research. Under excessive shearing, some microdefects will be created in Al 2024T3 due to particle cracking or microshear bands as shown in Figs.1 and 2. The dislocation density in the microshear bands is extremely high. The movement of dislocations is blocked and dislocation pileups will appear at certain locations. With an increase in the length of the dislocation pileups, some microcracks nucleate at those locations where dislocation pileups are intense, as shown in Fig.3. The nucleation, propagation and coalescence of microcracks should lead to material failure of the alloy. The shear damage-to-fracture process of the alloy has been illustrated by Fig.4. A true shear stress-strain curve of Al 2024T3 obtained from the in-situ single shear tests[11] in mesoscale is shown in Fig.5. The values of shear strain corresponding to the initiation of particle cracking, microshear banding and microcracking found from the curve are 2.12%, 14.98% and 31.62%,

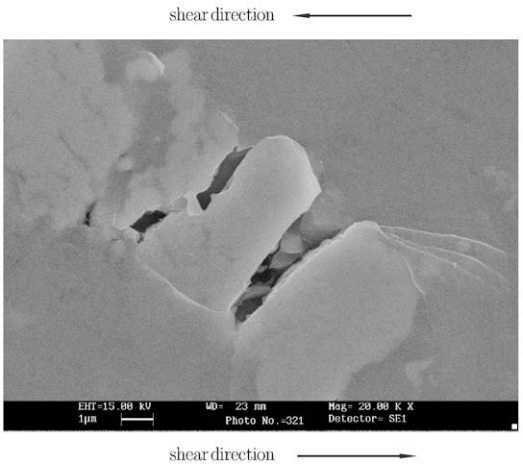

Fig. 1. Particle cracking and breaking.

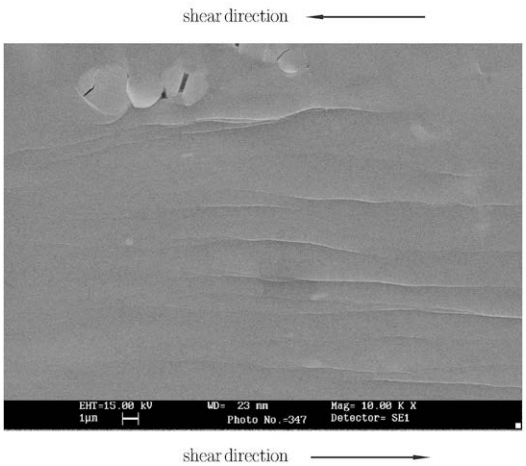

Fig. 2. Microshear banding in Al matrix.

respectively. The shear stress reaches almost the maximum value when microcracks appear. From these microscopic observations, the shear damage mechanism of Al 2024T3 may be regarded as a multi-stage damage process.

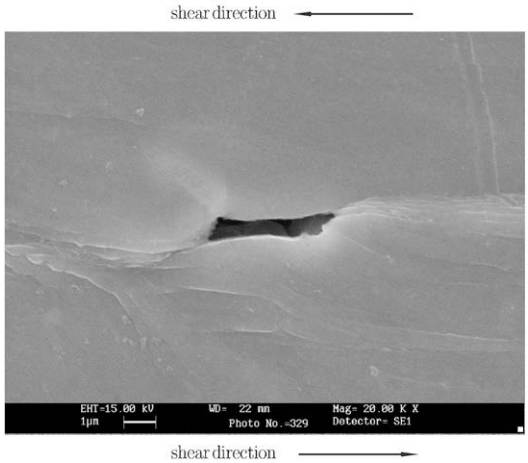

Fig. 3. Microcracking in Al matrix.

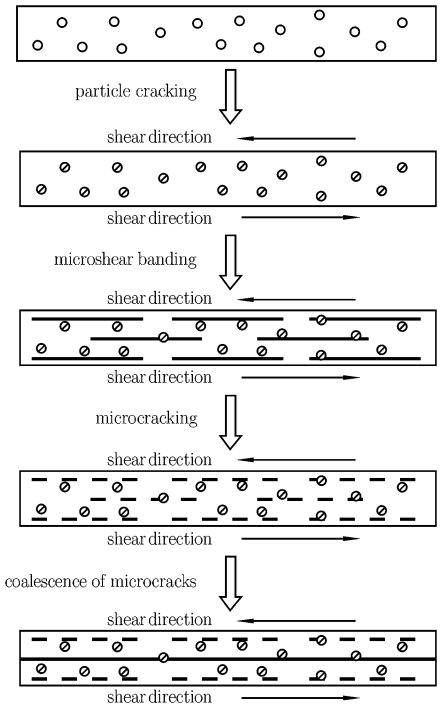

Fig. 4. The evolution of shear damage in Al 2024T3 (adopted from Ref.[11]).

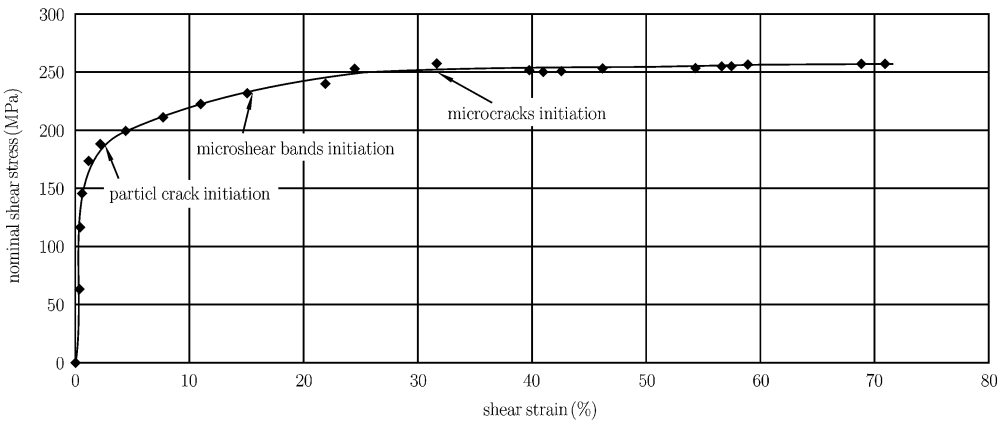

Fig. 5. Shear stress-strain curve of a single shear specimen.

III. DEFINITION OF SHEAR DAMAGE

Although damage could be anisotropic, metal damage is generally accepted to be isotropic. In this study, it is assumed that the virgin material and the damaged material are both isotropic. The isotropic damaged tensor $\boldsymbol{D}$ consists of two independent components, D_1 and D_2. This denotes that the state of

isotropic damage is described by two scalar damage parameters. The expressions of the two independent damage parameters[7, 12] are adopted as:

$$D_K = 1 - \frac{\tilde{K}}{K} \tag{1}$$

$$D_S = 1 - \frac{\tilde{G}}{G} \tag{2}$$

where K and $\tilde{K}$ are the bulk moduli of the virgin material and the damaged material, and G and $\tilde{G}$ are the shear moduli of the virgin material and the damaged material, respectively. D_K and D_S can be expressed separately as:

$$D_K = 1 - \frac{\sigma_m}{\tilde{\sigma}_m} \tag{3}$$

$$D_S = 1 - \frac{\sigma_{ij}}{\tilde{\sigma}_{ij}} \qquad (i \neq j \quad \text{no sum for } i, j) \tag{4}$$

where σ_{ij}, $\tilde{\sigma}_{ij}$, σ_m and $\tilde{\sigma}_m$ are the shear stress, the effective shear stress, the mean normal stress and the effective mean normal stress, respectively. From Eqs.(3) and (4), D_K is the damage due to the volume change of the representative volume element (RVE) and D_S is the damage due to the shape change of RVE. Therefore, D_K and D_S may be referred to as the dilatational damage variable and the shear damage variable, respectively. It is usually no volume change in pure shear deformation, therefore only shear damage is considered as follows.

The region between the two notches of a single shear specimen (Fig.6) is regarded as a pure shear zone for this formulation. Within the RVE (Fig.7), the shear damage D_s may be defined as:

$$D_S = 1 - \frac{A_D}{A} \tag{5}$$

where A is the apparent cross-sectional area of the RVE, and A_D is the effective shear load bearing area of the RVE.

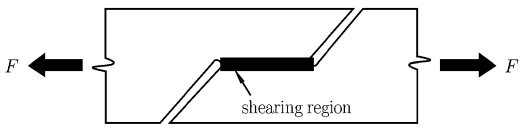

Fig. 6. The shearing region in a single shear specimen.

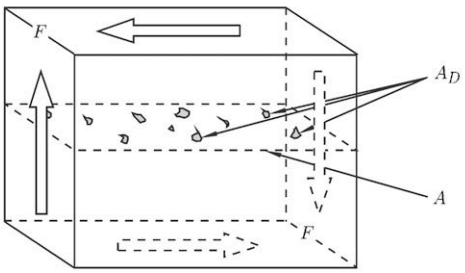

Fig. 7. A RVE subjected to pure shear.

The nominal shear stress τ and the effective shear stress $\tilde{\tau}$ can be written respectively as:

$$\tau = \frac{F}{A} \qquad \text{and} \qquad \tilde{\tau} = \frac{F}{A_D} \tag{6}$$

From Eqs.(5) and (6), the shear damage variable can hence be expressed as:

$$D_S = 1 - \frac{\tau}{\tilde{\tau}} \tag{7}$$

In general, the shear stress-strain relation of a given strain-hardening material may be described by the combination of a linear equation and a power-law equation:

$$\tau = G\gamma \quad \text{for} \quad \gamma \leq \gamma_y \tag{8}$$

and

$$\tau = k\gamma^n \quad \text{for} \quad \gamma \geq \gamma_y \tag{9}$$

where k and n are the material constants; γ_y is the shear yield strain.

Based on the hypothesis of strain equivalence[14], for the RVE of a damaged material, the shear constitutive relation can be written as:

$$\tilde{\tau} = k_0\gamma^{n_0} \quad \text{for} \quad \gamma \geq \gamma_y \tag{10}$$

where $\tilde{\tau}$ is the effective shear stress, while n_0 and k_0 are the hardening parameter and strength parameter for the undamaged material RVE. From Eqs.(9) and (10), together with Eq.(7), the shear damage variable can be expressed as:

$$D_S = 1 - \left(\frac{k}{k_0}\right)\gamma^{n-n_0} \tag{11}$$

From Eq.(11), it is found that the value of the shear damage is dependent on the decrement in both the material hardening parameter n and the material strength parameter k. Therefore, the macroscopic response of softening in the metal is caused by the mesoscopic shear damage in the material.

IV. EVOLUTION OF SHEAR DAMAGE AND DISCUSSIONS

4.1. Damage Evolution in a Shear Band

Before final rupture, the deformation-damage-failure process of Al 2024T3 may be divided into five stages (Fig.8) based on the in-situ microscopic observations of the shear bands[11]: (1) elastic deformation (OA); (2) elasto-plastic deformation without damage (AB); (3) elasto-plastic deformation with damage due to particle cracking (BC); (4) elasto-plastic deformation with damage due to the occurence of microshear bands (CD); and (5) elasto-plastic deformation with inclusion of particle cracking, microshear banding and microcracking in Al matrix (DE).

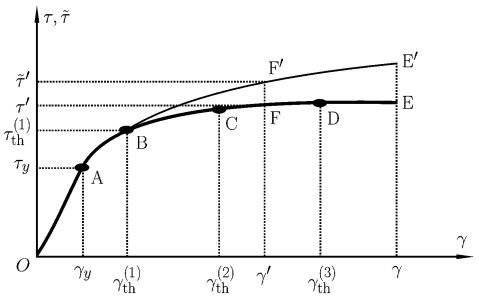

Fig. 8 Shear stress-strain curve in shear band.

Figure 8 also illustrates the mechanical response of the alloy from different damage mechanisms. Similar to Eq.(9), the shear stress-strain relation of the damaged material in the elasto-plastic-damage stage may be described by:

$$\tau = k_i\gamma^{n_i} \qquad (i = 1, 2, 3 \quad \text{for} \quad \gamma_{\text{th}}^{(i)} \leq \gamma \leq \gamma_{\text{th}}^{(i+1)}) \tag{12}$$

where, $\gamma_{\text{th}}^{(i)}$ $(i = 1, 2, 3)$ are the damage threshold shear strains for the initiation of particle cracking, microshear banding and microcracking, respectively.When the shear strain reaches its ultimate value, $\gamma_{\text{th}}^{(4)} = \gamma_c$. The material parameters k_i and n_i can be determined by the following equations for the four stages:

$$n_i = \frac{\ln(\tau_{\text{th}}^{(i+1)}) - \ln(\tau_{\text{th}}^{(i)})}{\ln(\gamma_{\text{th}}^{(i+1)}) - \ln(\gamma_{\text{th}}^{(i)})} \qquad (i = 0, 1, 2, 3) \tag{13}$$

$$k_i = \frac{\tau_{\text{th}}^{(i)}}{(\gamma_{\text{th}}^{(i)})^{n_i}} \qquad (i = 0, 1, 2, 3) \tag{14}$$

where, $\tau_{th}^{(i)}$ $(i = 0, 1, 2, 3)$ are the threshold shear stresses corresponding to $\gamma_{\text{th}}^{(i)}$ $(i = 0, 1, 2, 3)$, respectively; and $\tau_{\text{th}}^{(0)} = \tau_y$, $\gamma_{\text{th}}^{(0)} = \gamma_y$.

Using Eqs.(11) and (12), the shear damage variable can be determined for various stages as:

$$D_S^{(i)} = 0 \quad (i = 0, 1) \qquad \text{and} \qquad D_S^{(i+2)} = 1 - (\frac{k_i}{k_0})\gamma^{n_i - n_0} \quad (i = 0, 1, 2) \tag{15}$$

where $D_S^{(j)}$ is the shear damage value in the j-th stage. Suppose BF'E' represents the effective shear stress-strain curve ($\tilde{\tau}$-γ relation). F' is an arbitrary point in the elasto-plastic stage with damage. To determine n_0 and k_0, at points B and F', it can be calculated from Eqs.(10) and (15) that:

$$\tau_{\rm th}^{(1)} = k_0(\gamma_{\rm th}^{(1)})^{n_0} \tag{16}$$

$$1 - \left(\frac{k_i}{k_0}\right)\gamma^{n_i - n_0} = D_{S0} \tag{17}$$

where D_{S0} is the shear damage value for a specific value of the shear strain $\gamma = \gamma'$ (Fig.8) and can be obtained by measuring the effective shear modulus $\tilde{G}$. Hence, from Eqs.(16) and (17), we can obtain the formulae for the parameters n_0 and k_0:

$$n_0 = \frac{\ln(k_i) + n_i\ln(\gamma_0) - \ln(k_1) - n_1\ln(\gamma_{\rm th}^{(1)}) - \ln(1 - D_{S0})}{\ln(\gamma_0) - \ln(\gamma_{\rm th}^{(1)})} \tag{18}$$

$$k_0 = \frac{\tau_{\rm th}^{(1)}}{(\gamma_{\rm th}^{(1)})^{n_0}} \tag{19}$$

4.2. The Evolution of Shear Damage in Al 2024T3

In Ref.[13], torsion tests have been used to measure the shear damage values versus the shear strain for Al 2024T3 and the results obtained are listed in Table 1. Using Eqs.(13) and (14) and these data together with those in Fig.5, the material parameters are estimated and listed in Table 2. Furthermore, the parameters n_0 and k_0 are also estimated by Eqs.(18) and (19) and listed in Table 2. The apparent stress-strain curve, the effective stress-strain curve, and the shear damage evolution curve are hence plotted in Fig.9.

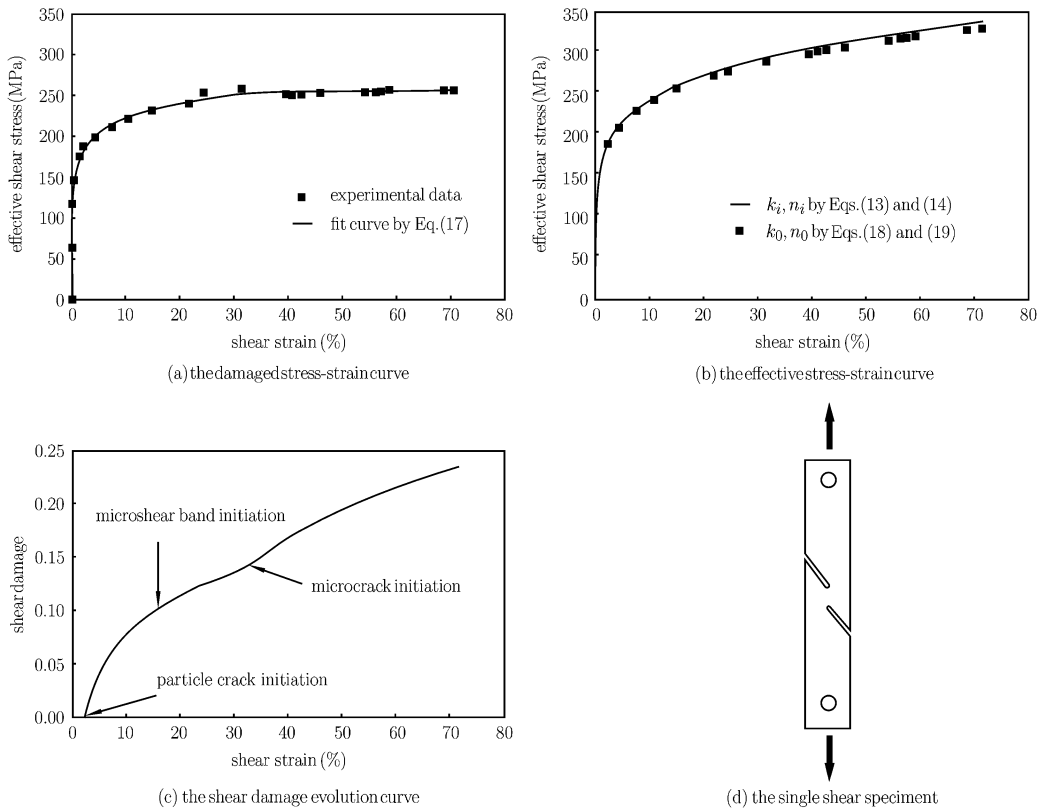

Fig. 9. The damaged stress-strain curve, the effective stress-strain curve, the shear damage evolution curve in a shear band and the single shear specimen.

Table 1. **The shear damage versus the shear strain for Al 2024T3**

γ (%)	0	1.37	2.5	4.01	5.91	8.19	10.88
D_S	0	0.041	0.0409	0.0465	0.057	0.057	0.059

Table 2. **Material Parameters of Al 2024T3**

i	0 [Eqs.(13, 14)]	0 [Eqs.(18, 19)]	1	2	3
n_i	0.169228	0.163071	0.112922	0.107997	0.023196
k_i	356.6252	348.5296	289.0738	286.3839	259.7450

4.3. The Effect of Morphological Changes on the Shear Damage of Al 2024T3

After cracking of the intermetallic particles in the shear band to commence, the load borne by them is gradually transferred to the surrounding matrix in mesoscale. In this case, the shear damage induced by particle cracking remains constant in macroscale. When the shear damage in the microshear bands reaches a critical value, microcracks in the matrix initiate near the grain boundaries. Mild increment of the shear damage value mainly results from the matrix microcracking instead of the formation of microshear bands. The value of the shear damage due to different micro-morphological changes is shown in Fig.10. The values of the shear damage due to particle cracking, microshear banding and matrix microcracking are denoted by $D_S^{(pc)}$, $D_S^{(mb)}$ and $D_S^{(mc)}$, respectively. They are expressed as:

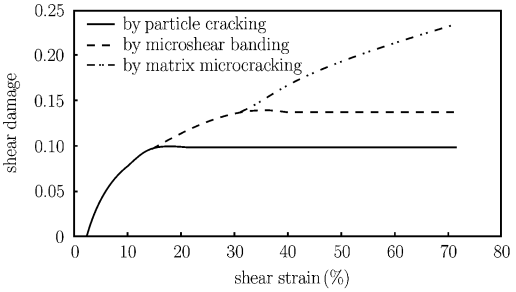

Fig. 10 Path of J-integral around the crack tip.

$$\begin{aligned} D_S^{(pc)} &= D^{(3)} && \text{for} \quad \gamma \geq \gamma_{\text{th}}^{(1)} \\ D_S^{(mb)} &= D^{(4)} - D_S^{(pc)} && \text{for} \quad \gamma \geq \gamma_{\text{th}}^{(2)} \\ D_S^{(mc)} &= D^{(4)} - (D_S^{(pc)} + D_S^{(mb)}) && \text{for} \quad \gamma \geq \gamma_{\text{th}}^{(3)} \end{aligned} \tag{20}$$

where

$$\begin{aligned} D_S^{(1)} &= D^{(2)} = 0 && \text{for} \quad \gamma \leq \gamma_{\text{th}}^{(1)} \\ D_S^{(3)} &= 1 - \left(\frac{k_1}{k_0}\right) \gamma^{n_1 - n_0} && \text{for} \quad \gamma_{\text{th}}^{(2)} \geq \gamma \geq \gamma_{\text{th}}^{(1)} \\ D_S^{(3)} &= 1 - \left(\frac{k_1}{k_0}\right) (\gamma_{\text{th}}^{(2)})^{n_1 - n_0} && \text{for} \quad \gamma \geq \gamma_{\text{th}}^{(2)} \\ D_S^{(4)} &= 1 - \left(\frac{k_2}{k_0}\right) \gamma^{n_2 - n_0} && \text{for} \quad \gamma_{\text{th}}^{(3)} \geq \gamma \geq \gamma_{\text{th}}^{(2)} \\ D_S^{(4)} &= 1 - \left(\frac{k_2}{k_0}\right) (\gamma_{\text{th}}^{(3)})^{n_2 - n_0} && \text{for} \quad \gamma \geq \gamma_{\text{th}}^{(3)} \\ D_S^{(4)} &= 1 - \left(\frac{k_3}{k_0}\right) \gamma^{n_3 - n_0} && \text{for} \quad \gamma \geq \gamma_{\text{th}}^{(3)} \end{aligned} \tag{21}$$

Compared with Fig.9(c), the outer envelope of the three curves in Fig.10 is simply the accumulated damage evolution curve of the alloy under shearing.

For isotropic materials, either virgin or damaged, two independent material parameters have been used to describe their elasto-plastic behaviors. Therefore, isotropic damage may be described by two damage scalar variablesD_K and D_S[7, 14]. The shear damage variable D_S has been adopted to quantify the damage of Al 2024T3 under shearing. Figure 5 illustrates that the morphological changes in the microstructure lead to softening of the alloy. Hence, the material hardening parameter n and the material strength parameter k are reduced. The curve AB in Fig.8 can be used to theoretically determine parameters n_0 and k_0 by using Eqs.(13) and (14). However, the strain range in the elasto-plastic stage without damage is usually small. In the calculation of n_0 and k_0, the uncertainty of experimental data in this stage is sensitive to the accuracy.

Alternatively, Eqs.(18) and (19) can be also used for determining the parameters n_0 and k_0. The damage variable D_{S0} can be obtained by measuring the change in the shear modulus. Since the damage definitions using the concept of effective stress and the change in elastic modulus are the same, the damage variable D_{S0} defined by the change in shear modulus can be substituted into Eq.(17) to evaluate the parameters n_0 and k_0.

V. CONCLUSIONS

The proposed formulation has been used to quantify the multi-stage shear damage evolution in shearing of Al 2024T3. A multi-stage damage evolution equation has been derived to describe the effect of shear damage under different types of microstructural change in the material. Material softening becomes a descriptor of the macroscopic response to the shear damage of the alloy. The formulation does not only denote the relation between the microstructural change and the macromechanical material response, but also bridges the gap between the concepts of the local mesoscale damage and the overall macroscale damage.

References

[1] Lemaitre,J.. Coulped elasto-plasticity and damage constructive equations. *Comput. Meth. Appl. Mech. Eng.*, 1985, 51: 31-49.

[2] Shi,M.Z.. Measuring the damage factor of materials with the thin-walled cylinder torsion test and the low-cycle fatigue test. *Eng. Fract. Mech.*, 1993, 44: 267-273.

[3] Tang,C.Y. and Lee,W.B.. Effects of damage on the shear modulus of aluminium alloy 2024T3. *Scripta Metallurgica et Materialia*, 1995, 32: 1993-1999.

[4] Lankford,J.. Shear versus Dilatational damage mechanisms in the compressive failure of fibre-reinforced composites. *Compos. Pt. A-Appl. Sci. Manuf.*, 1997, 28A: 215-222.

[5] Jepsen,K.J. and Davy,D.T., Comparison of damage accumulation measure in human cortical bone. *J. Biomech*, 1997, 30: 891-894.

[6] Li,G.Q., A flexibility approach for damage identification of cantilever-type structure with bending and shear deformation. *Comput. Struct.*, 1999, 73: 565-572.

[7] Cauvin,A. and Testa,R.B.. Damage mechanics: basic variables in continuum theories, *Int. J. Solids Struct.*, 1999, 36: 747-761.

[8] Cauvin,A. and Testa,R.B.. Elastoplastic material with isotropic damage. *Int. J. Solids Struct.*, 1999, 36: 727-746.

[9] Loland,K.E.. Continuous damage model for load-response estimation of concrete, *Cem. Concr. Res.*, 1980, 10: 395-402.

[10] Mazars,J.. Application de la mecanique de l'endommagement au comportment non lineare a la rupture du beton de structure, These de Doctorat d'Etat. Univ. P. Et M. Curie, Paris 6, France, 1984.

[11] Tang,C.Y., Lee,T.C., Rao,B. and Chow,C.L.. An experimental study of shear damage using in-situ shear test. *Int. J. Damage Mech.*, 2002, 11: 335-353.

[12] Lemaitre,J.. How to use damage mechanics. *Nucl. Eng. Des.*, 1984, 80: 233-246.

[13] Lee,T.C., Tang,C.Y. and Rao,B.. Microscopic observation and curve surface moire measurement of shear damage in aluminium alloy 2024T3. Proc. 9^{th} International Manufacturing Conference, China, 2000.

[14] Tang,C.Y., Shen,W., Peng,L.H. and Lee,T.C.. Characterization of Isotropic Damage Using Double Scalar Variables. *Int. J. Damage Mech.*, 2002, 11: 1-25